Journal of Guidance, Control, and Dynamics, Vol. 41, Issue 1, 2018, pp. 171-183
DOI:10.2514/1.G002949

Gravity Turn-Assisted Optimal Guidance Law

Shaoming He[a] and Chang-Hun Lee[b]
Cranfield University, Cranfield MK43 0AL, UK

This paper proposes a new optimal guidance law that directly utilizes, instead of compensating, the gravity for accelerating missiles. The desired collision triangle that considers both gravity and vehicle's axial acceleration is analytically derived based on geometric conditions. The concept of instantaneous zero-effort-miss is introduced to allow for analytical guidance command derivation. By formulating a finite-time instantaneous zero-effort-miss regulation problem, the proposed optimal guidance law is derived through Schwarz's inequality approach. The relationships of the proposed formulation with conventional proportional navigation guidance and guidance-to-collision are analyzed and the results show that the proposed guidance law encompasses previously suggested approaches. The significant contribution of the proposed guidance law lies in that it ensures zero final guidance command and enables energy saving with the aid of utilizing gravity turn. Nonlinear numerical simulations clearly demonstrate the effectiveness of the proposed approach.

I. Introduction

The well justified proportional navigation guidance (PNG) law [1–3] has been widely used for almost half a century in missile guidance system and is still a benchmark for new guidance law design. The PNG issues a lateral acceleration that is proportional to the line-of-sight (LOS) rate to steer the interceptor to fly along the collision triangle to hit the target. Using optimal control theory, Zarchan [1] proved that the PNG with navigation ratio 3 is energy optimal. Later in [4–6], the authors further revealed that the PNG with a constant navigation ratio is also an optimal

[a] PhD Candidate, School of Aerospace, Transport and Manufacturing, Email: shaoming.he.cn@gmail.com
[b] Research Fellow (Corresponding Author), School of Aerospace, Transport and Manufacturing, Email: chlee@fdcl.kaist.ac.kr

guidance law in the sense of time-to-go weighted energy optimal. The rational for using PNG lies in that it can force the zero-effort-miss (ZEM) to converge to zero in finite time to ensure target capture.

In PNG formulation, the assumptions of constant-speed vehicle and no gravity are required to derive the corresponding ZEM. For constant-speed vehicle, the resulting collision triangle is defined by straight lines whose lengths are proportional to the target's and pursuer's velocity. The constant-speed assumption simplifies the theoretical analysis and justifies the linearized kinematics model. In some cases, the vehicle's speed is slowly varying and therefore the constant-speed assumption is valid. However, when the interceptor is subject to large acceleration or deceleration, PNG cannot drive the missile to follow the desired straight line collision course and is far away from energy optimal [7, 8]. This is especially severe for exo-atmosphere interceptors and agile missiles, where high angle-of-attack maneuver is feasible. Assuming the missile velocity profile is known prior, the authors in [8] developed a new energy optimal guidance law, called guidance-to-collision (G2C), that guides the interceptor on a straight line collision course to approach the predicted interception point (PIP). The ZEM, formulated on the basis of constant axis accelerating missile and no gravity, was leveraged in the derivation of the G2C law. With the same collision triangle as in [8], the authors in [9] further suggested a sliding mode control (SMC) exo-atmospheric guidance law for accelerating missiles. Numerical simulations revealed that the SMC-based guidance law has larger capture zone than PNG. A new differential game guidance law was proposed in [10] for varying missile velocity model with bounded control limits. The energy optimal G2C for exo-atmospheric interception was studied in [11], which also considered the missile dynamics and intercept angle constraint in guidance law design.

Note that most previous guidance laws were proposed under the gravity-free assumption and utilized additional term $g\cos\gamma_M$ to counteract the effect of gravity in implementation. This simple compensating approach, obviously, cannot guarantee zero terminal guidance command in applications, leading to the sacrifice of operational margins. Additionally, direct gravity compensation requires extra energy. Motivated by these observations, this paper aims to propose a new gravity turn-assisted optimal guidance law that automatically utilizes the gravity instead of compensating

it for accelerating missiles. Our solution of this problem is to design a guidance law that optimally minimizes the ZEM considering gravity and vehicle's axial acceleration, thereby guiding the missile to follow a desired curved path to intercept the target. To the best of our knowledge, this may be the first time to introduce the gravity turn-assisted optimal guidance law.

The analytical collision triangle considering gravity and missile's axis acceleration is first derived. Unlike PNG and G2C, the resulting desired path defined by the collision triangle for our case is a curved trajectory instead of a straight line. On the basis of this geometric information, a new concept, called instantaneous ZEM, is introduced to make analytical guidance command derivation tractable. Detailed analysis shows that the proposed instantaneous ZEM reduces to PNG-type ZEM when ignoring both the axis acceleration and gravity, and G2C-type ZEM when neglecting the effect of gravitational acceleration. The proposed optimal guidance law is then derived by solving a linear quadratic optimal control problem through Schwarz's inequality approach. We further show that the conventional PNG and G2C are all special cases of the proposed guidance law. The advantages of the proposed approach are clear: guaranteeing zero final guidance command and saving energy without requiring extra control effort to compensate the gravity. We also reveal that the proposed guidance law can be easily extended to intercept angle control by adding an additional biased term.

The rest of the paper is organized as follows. Sec. II presents some preliminaries and backgrounds. Sec. III provides the details the ideal collision triangle derivation, followed by the proposed optimal guidance law shown in Sec. IV. Finally, some simulation results and conclusions are offered.

II. Preliminaries and Backgrounds

In this section, we first present the missile-target kinematics models, including exo-atmospheric and endo-atmospheric, for later use in guidance law design. The problem formulation is then stated to clearly demonstrate the motivation and objective of this paper. Before introducing the system kinematics and the proposed method, we make two basic assumptions as follows:

Assumption 1. Both the interceptor and the target are assumed as point-mass models.

Assumption 2. The engagement occurs in a 2-D vertical plane.

Note that these assumptions are widely accepted in guidance law design for tactical missiles: (Assumption 1) Typical philosophy treats the guidance and control loops separately by placing the

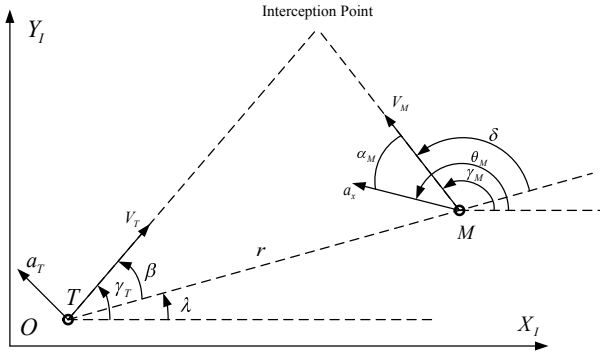

Fig. 1 Planar geometry of homing engagement.

kinematic guidance system in an outer-loop, generating guidance commands tracked by an inner dynamic control loop, also known as autopilot. (Assumption 2) Homing engagement can be treated as a 2-D problem and gravity compensation is in the vertical plane.

A. Model Derivation

It is assumed that the interceptor employs an ideal attitude control system that provides roll stabilization such that the guidance problem can be treated in two separate channels. Fig. 1 shows the planar homing engagement geometry in this study, where M and T denote the missile and target, respectively. The notation of (X_I, Y_I) represents the inertial frame. The variables of λ and γ stand for the LOS angle and flight path angle. r denotes the relative distance between the target and the missile. a and V are the acceleration and velocity of the vehicles. θ_M is the missile's body angle. The missile angle-of-attack and axial acceleration are denoted by α_M and a_x, respectively. Note that α_M is known as the shear angle to represent the angle between the velocity vector and thrust vector for exo-atmospheric vehicles [12]. In order to allow for a closed-form formulation, we assume that the missile's axial acceleration a_x is constant. Note that this assumption is widely-accepted in guidance law design for accelerating missiles [7–10].

The corresponding equations describing the missile-target relative motion are formulated as

$$\dot{r} = V_r \tag{1}$$

$$r\dot{\lambda} = V_\lambda \tag{2}$$

where the relative speeds along and perpendicular to the LOS are

$$V_r = V_M \cos\delta - V_T \cos\beta \tag{3}$$

$$V_\lambda = V_M \sin\delta - V_T \sin\beta \tag{4}$$

The complementary equations that describe the relationship between the lead angle and flight path angle are

$$\delta = \gamma_M - \lambda \tag{5}$$

$$\beta = \gamma_T - \lambda \tag{6}$$

For simplicity, it is also assumed that the target is moving with constant speed and employs a lateral maneuver to change its course as

$$\dot{\gamma}_T = \frac{a_T}{V_T} \tag{7}$$

B. Exo-Atmospheric Interception

During the exo-atmospheric endgame, it is assumed that the interceptor has a constant axial acceleration a_x provided by a mounted rocket motor. The missile employs controllable thrusters to change the attitude and consequently uses this acceleration in the required direction. Attitude control system based on thrusters can direct the axial acceleration vector to the desired direction to provide both trajectory shaping and energy increase [9]. It is assumed that the attitude dynamics are ideal, i.e. the desired attitude is obtained with no time delays. Due to the missile's acceleration, the flight path angle and speed evolve according to

$$\dot{\gamma}_M = \frac{a_x \sin\alpha_M - g\cos\gamma_M}{V_M} \tag{8}$$

$$\dot{V}_M = a_x \cos\alpha_M - g\sin\gamma_M \tag{9}$$

where g stands for the gravitational acceleration.

As can be observed from (8), the change rate of the flight path angle is resulted from two factors, the shear angle term $a_x \sin\alpha_M$ and gravitational effect $g\cos\gamma_M$. Since the duration of the terminal

guidance phase is typically very short, we assume that the gravitational acceleration g is constant in guidance law design.

Motivated by the concept of G2C, the control interest for exo-atmospheric interception is to design a guidance law to nullify the initial heading errors such that the interceptor maintains its acceleration vector in the direction of its velocity vector thereafter. Consequently, if the target has no maneuvers, the missile will fly along an ideal trajectory that requires no extra control effort to the expected collision point. This characteristic is of great importance to kinematic kill vehicles (KKVs) since this strategy can reduce the magnitude of interceptor's shear angle and therefore significantly increase the kill probability [9]. To realize this, the key part is to find the closed-form solution of an ideal collision triangle for the missile that requires no extra control effort, i.e. $\alpha_M = 0$. Once we have the closed-form solution, we can easily design a guidance law that drives the missile trajectory to converge to the ideal collision triangle in finite time. For notation simplicity, let $a_M = a_x \sin\alpha_M$ be the virtual control input for exo-atmospheric case.

C. Endo-Atmospheric Interception

In an endo-atmospheric engagement, the missile is usually controlled by aerodynamic forces. Let a_M be the acceleration that is perpendicular to the missile's velocity vector. Then, the dynamics of flight path angle and flight velocity are governed by

$$\dot{\gamma}_M = \frac{a_M - g\cos\gamma_M}{V_M} \tag{10}$$

$$\dot{V}_M = a_x - g\sin\gamma_M \tag{11}$$

Similar to exo-atmospheric case, our aim is to find the ideal collision triangle for the interceptor that requires no extra control effort, i.e. $a_M = 0$. As can be noted from (10) and (11), if we enforce $a_x = g = 0$, the system model reduces to the constant velocity model that is widely-used in guidance law design; if $g = 0$, the system model becomes constant accelerating model that is used in endo-atmospheric G2C law design [8]. Consequently, our model is a more general one that approximates the practical situations at most.

D. Problem Formulation

Most previous works assumed no gravity when designing terminal guidance laws and leveraged additional add-on term $g\cos\gamma_M$ to reject the effect of gravity in implementation. This straightforward approach works well in practical applications but has two main drawbacks. On one hand, compensating gravity using extra term $g\cos\gamma_M$ means that the terminal guidance command cannot converge to zero, leading to the sacrifice of operational margins. On the other hand, the additional term may require more energy for gravity compensation. In order to address these two problems, the objective of this paper is to propose a new gravity turn-assisted optimal guidance law that automatically utilizes the gravity instead of compensates it for accelerating missiles.

III. Collision Triangle Derivation

This section derives the closed-form solution of the proposed ideal collision triangle in the presence of gravity. Once we obtain the ideal collision triangle, we can utilize the optimal control theory to design a guidance law that forces to missile to fly along the collision triangle to achieve the design goal.

Definition 1. The ideal motion of the interceptor is defined as the missile kinematics with zero control input.

In the derivation of the desired collision triangle, it is natural to enforce the condition of the ideal motion of the interceptor, that is, $\alpha_M = 0$ for exo-atmospheric case or $a_M = 0$ for endo-atmospheric case as our goal is to make the terminal guidance command converge to zero. Under this condition, the missile's kinematics, when on the ideal collision triangle, is formulated as

$$\dot{x}_M = V_M\cos\gamma_M \tag{12}$$

$$\dot{y}_M = V_M\sin\gamma_M \tag{13}$$

$$\dot{\gamma}_M = -\frac{g\cos\gamma_M}{V_M} \tag{14}$$

$$\dot{V}_M = a_x - g\sin\gamma_M \tag{15}$$

where (x_M, y_M) represents the inertial position of the interceptor.

It follows from (12)-(15) that these four differential equations are dependent on the flight path angle γ_M and direct integration seems to be intractable. From the point of problem dimension reduction, we manually change the argument from time t to flight path angle γ_M. Then, (12)-(15) can be reformulated as

$$\frac{dt}{d\gamma_M} = -\frac{V_M}{g\cos\gamma_M} \tag{16}$$

$$\frac{dx_M}{d\gamma_M} = \frac{dx_M}{dt}\frac{dt}{d\gamma_M} = -\frac{V_M^2}{g} \tag{17}$$

$$\frac{dy_M}{d\gamma_M} = \frac{dy_M}{dt}\frac{dt}{d\gamma_M} = -\frac{V_M^2}{g}\tan\gamma_M \tag{18}$$

$$\frac{dV_M}{d\gamma_M} = \frac{dV_M}{dt}\frac{dt}{d\gamma_M} = V_M\tan\gamma_M - \frac{a_x V_M}{g\cos\gamma_M} \tag{19}$$

Through this argument changing, we only need to solve three independent differential equations to find the analytical solution. This will be shown in the following parts.

Assumption 3. The flight path angle γ_M satisfies $\gamma_M \in (-\pi/2, \pi/2)$. In implementation, the variation of the flight path angle during terminal guidance phase is limited and thus Assumption 3 can be ensured by using coordinate transformation.

Let $\kappa = -a_x/g$, then, (19) can be rewritten as

$$\frac{dV_M}{d\gamma_M} = V_M\tan\gamma_M + \frac{\kappa V_M}{\cos\gamma_M} \tag{20}$$

which is equivalent to

$$\frac{dV_M}{V_M} = \left(\tan\gamma_M + \frac{\kappa}{\cos\gamma_M}\right)d\gamma_M \tag{21}$$

Imposing integration on both sides of (21) under Assumption 1 gives

$$\ln V_M(\gamma_M)\big|_{\gamma_{M0}}^{\gamma_{Mf}} = -\ln\cos\gamma_M\big|_{\gamma_{M0}}^{\gamma_{Mf}} + \kappa\ln(\sec\gamma_M + \tan\gamma_M)\big|_{\gamma_{M0}}^{\gamma_{Mf}} \tag{22}$$

where γ_{Mf} and γ_{M0} denote the final and initial flight path angles, respectively.

Solving (22) for $V_M(\gamma_{Mf})$ yields

$$V_M(\gamma_{Mf}) = C\sec\gamma_{Mf}(\sec\gamma_{Mf} + \tan\gamma_{Mf})^{\kappa} \tag{23}$$

where $C = \frac{V_M(\gamma_{M0})}{\sec\gamma_{M0}(\sec\gamma_{M0}+\tan\gamma_{M0})^{\kappa}}$ is the integration constant, determined by the initial conditions.

Setting γ_{Mf} as γ_M and substituting (23) into (16)-(18) results in

$$\frac{dt}{d\gamma_M} = -\frac{C}{g}\sec^2\gamma_M\left(\sec\gamma_M+\tan\gamma_M\right)^{\kappa} \tag{24}$$

$$\frac{dx_M}{d\gamma_M} = -\frac{C^2}{g}\sec^2\gamma_M\left(\sec\gamma_M+\tan\gamma_M\right)^{2\kappa} \tag{25}$$

$$\frac{dy_M}{d\gamma_M} = -\frac{C^2}{g}\sec^2\gamma_M\tan\gamma_M\left(\sec\gamma_M+\tan\gamma_M\right)^{2\kappa} \tag{26}$$

Following the detailed derivations shown in Appendix A, we have the closed-form solution as

$$t\left(\gamma_M\right) = t\left(\gamma_{M0}\right) - \frac{C}{g}\left[f_t\left(\gamma_M\right) - f_t\left(\gamma_{M0}\right)\right] \tag{27}$$

$$x_M\left(\gamma_M\right) = x_M\left(\gamma_{M0}\right) - \frac{C^2}{g}\left[f_x\left(\gamma_M\right) - f_x\left(\gamma_{M0}\right)\right] \tag{28}$$

$$y_M\left(\gamma_M\right) = y_M\left(\gamma_{M0}\right) - \frac{C^2}{g}\left[f_y\left(\gamma_M\right) - f_y\left(\gamma_{M0}\right)\right] \tag{29}$$

where

$$f_t\left(\gamma_M\right) = \frac{1}{\kappa^2-1}\left(\kappa\sec\gamma_M-\tan\gamma_M\right)\left(\sec\gamma_M+\tan\gamma_M\right)^{\kappa} \tag{30}$$

$$f_x\left(\gamma_M\right) = \frac{1}{4\kappa^2-1}\left(2\kappa\sec\gamma_M-\tan\gamma_M\right)\left(\sec\gamma_M+\tan\gamma_M\right)^{2\kappa} \tag{31}$$

$$f_y\left(\gamma_M\right) = \frac{1}{4\kappa^2-4}\left(2\kappa\sec\gamma_M\tan\gamma_M-\tan^2\gamma_M-\sec^2\gamma_M\right)\left(\sec\gamma_M+\tan\gamma_M\right)^{2\kappa} \tag{32}$$

Setting $\gamma_{M0} = \gamma_M$ and $\gamma_M = \gamma_{Mf}$ in (27)-(29) provide the ideal motion of the interceptor that requires no extra control effort as

$$t\left(\gamma_{Mf}\right) = t\left(\gamma_M\right) - \frac{C}{g}\left[f_t\left(\gamma_{Mf}\right) - f_t\left(\gamma_M\right)\right] \tag{33}$$

$$x_M\left(\gamma_{Mf}\right) = x_M\left(\gamma_M\right) - \frac{C^2}{g}\left[f_x\left(\gamma_{Mf}\right) - f_x\left(\gamma_M\right)\right] \tag{34}$$

$$y_M\left(\gamma_{Mf}\right) = y_M\left(\gamma_M\right) - \frac{C^2}{g}\left[f_y\left(\gamma_{Mf}\right) - f_y\left(\gamma_M\right)\right] \tag{35}$$

In order to derive the conditions for the collision triangle, one needs to find the predicted interception point (PIP). As the target acceleration is usually difficult to obtain in advance, we

assume that the target adopts a gravity compensation scheme with constant flying velocity in collision triangle derivation. With this in mind, the terminal position of the target after t_{go} is given by

$$x_T(t_f) = x_T + V_T \cos\gamma_T t_{go} = x_M + r\cos\lambda + V_T \cos\gamma_T t_{go} \tag{36}$$

$$y_T(t_f) = y_T + V_T \sin\gamma_T t_{go} = y_M + r\sin\lambda + V_T \sin\gamma_T t_{go} \tag{37}$$

where $t_f = t + t_{go}$ denotes the final impact time.

From (33), the time-to-go t_{go} can be formulated as

$$t_{go} = t(\gamma_{Mf}) - t(\gamma_M) = -\frac{C}{g}\left[f_t(\gamma_{Mf}) - f_t(\gamma_M)\right] \tag{38}$$

A perfect interception requires

$$x_M(t_f) = x_T(t_f) \tag{39}$$

$$y_M(t_f) = y_T(t_f) \tag{40}$$

Equations (34)-(40) define the ideal instantaneous collision triangle considering gravity that requires no extra control effort for the missile to intercept the target.

Remark 1. If one can accurately estimate the target maneuver using a well-tuned filter, (36) and (37) can be replaced with

$$\begin{aligned} x_T(t_f) &= x_T + \textstyle\int_t^{t_f} V_T \cos\gamma_T(\tau)\, d\tau \\ &= x_T + V_T \textstyle\int_t^{t_f} \cos\left[\gamma_T + \omega(\tau - t)\right] d\tau \\ &= x_M + r\cos\lambda + \tfrac{V_T}{\omega}\sin(\gamma_T + \omega t_{go}) - \tfrac{V_T}{\omega}\sin\gamma_T \end{aligned} \tag{41}$$

$$\begin{aligned} y_T(t_f) &= y_T + \textstyle\int_t^{t_f} V_T \sin\gamma_T(\tau)\, d\tau \\ &= y_T + V_T \textstyle\int_t^{t_f} \sin\left[\gamma_T + \omega(\tau - t)\right] d\tau \\ &= y_M + r\sin\lambda - \tfrac{V_T}{\omega}\cos(\gamma_T + \omega t_{go}) + \tfrac{V_T}{\omega}\cos\gamma_T \end{aligned} \tag{42}$$

where $\omega = \dot{\gamma}_T = a_T/V_T$ denotes the flight path angle turning rate of the target.

Remark 2. In previous derivations, we utilize the widely-accepted assumptions that the target adopts a gravity compensation scheme and maintains constant flying velocity. For ballistic targets

with no gravity compensation, one can include the gravitational effect in target position prediction to obtain more accurate PIP. This can be easily achieved in a similar way as (28)-(29) by setting $\kappa = 0$.

IV. Optimal Guidance Law Design and Analysis

In this section, the concept of instantaneous ZEM considering gravity is first introduced and a new optimal guidance law is proposed to drive the instantaneous ZEM to converge to zero in finite time. We then analyze the relationships between our approach and some previous guidance laws and finally extend the proposed guidance law to intercept angle control.

A. Instantaneous Zero-Effort-Miss

Substituting (34)-(38) into (39)-(40) and using the relationships (30)-(32), one can obtain two coupled equalities, which are functions of the current and final flight path angles, as

$$f_1\left(\gamma_M, \gamma_{Mf}\right) = 0, \quad f_2\left(\gamma_M, \gamma_{Mf}\right) = 0 \tag{43}$$

Due to the complicated forms of $f_1\left(\gamma_M, \gamma_{Mf}\right)$ and $f_2\left(\gamma_M, \gamma_{Mf}\right)$, it is difficult to find the analytical solutions of γ_M and γ_{Mf}. However, the exact roots of the two coupled equations in (43) at each time instant during the terminal homing phase can be easily obtained through some well-known numerical algorithms, such as trust-region algorithm [13] and levenberg-marquardt algorithm [14]. Let the two roots of (43) at the current time be γ^* and γ_f^*, where γ^* denotes the desired current flight path angle and γ_f^* represents the desired terminal flight path angle.

Assumption 4. Since the flight path angle is slowly varying, we assume that γ^* is piece-wise constant, e.g. $\dot{\gamma}^* = 0$, in guidance law design.

It is well-known that forcing the missile to fly along the collision triangle requires regulating the corresponding ZEM to converge to zero. Recall that the original ZEM is defined as the final miss distance to the desired final interception course if both the pursuer and the target do not perform any maneuver from the current time instant onward [1], finding the analytic dynamics of the original ZEM is intractable for the curved trajectory due to gravity. To address this problem, we introduce a new concept, called instantaneous ZEM, which is defined on the basis of straight line trajectory at each time instant.

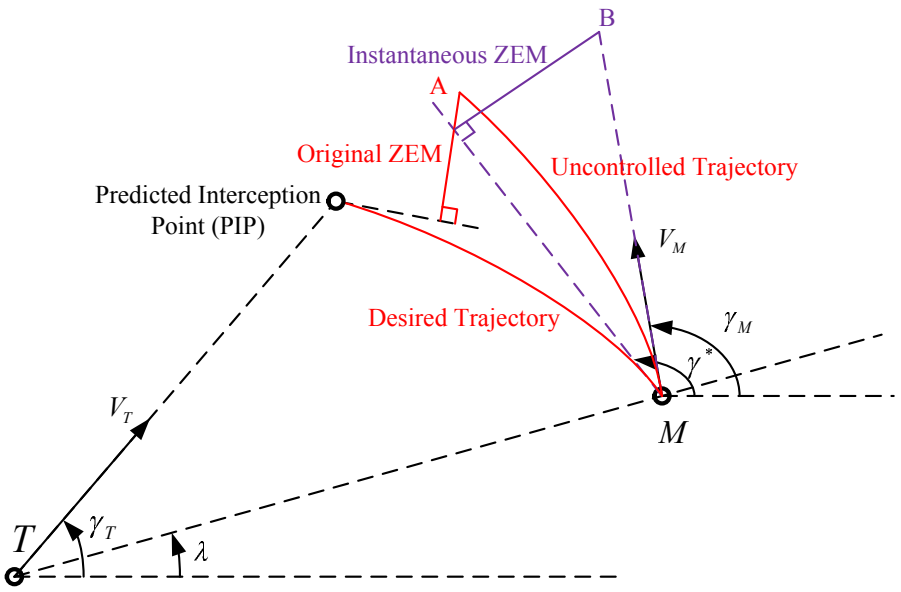

Fig. 2 Definition of instantaneous ZEM.

Definition 2. The instantaneous ZEM is defined as the final distance the missile would miss the target if the target continues along its present course and the missile follows a straight line along its current flight path angle with no further corrective maneuvers.

The geometric interpretation of the proposed instantaneous ZEM is shown in Fig. 2, where the curved path $M-PIP$ is the desired trajectory, $M-A$ the uncontrolled flight path from the current time onward and the straight line $M-B$ the instantaneous uncontrolled flight trajectory. According to the concept of instantaneous ZEM, the travelled length of $M-B$ is given by $V_M t_{go} + 0.5 a_x t_{go}^2$. Let $e_\gamma = \gamma_M - \gamma^*$ be the flight path angle error and z be the instantaneous ZEM. Obviously, one can note that if the instantaneous ZEM converges to zero, the flight path angle error e_γ converges to zero. This also means that the original ZEM converges to zero and therefore the interceptor will follow the desired collision triangle to hit the target. From Fig. 2, one can directly derive the instantaneous ZEM as

$$z = -\sin(e_\gamma)\left(V_M t_{go} + \frac{1}{2} a_x t_{go}^2\right) \tag{44}$$

Under small angle assumption of e_γ, the first-order time derivative of the instantaneous ZEM can be approximated by the length of $M-B$ times the angular rotating speed $\dot{e}_\gamma$ as

$$\dot{z} = -\dot{e}_\gamma\left(V_M t_{go} + \frac{1}{2} a_x t_{go}^2\right) = -a_M\left(t_{go} + \frac{a_x}{2V_M} t_{go}^2\right) \tag{45}$$

where the kinematics equation $\dot{\gamma} = a_M/V_M$ and Assumption 4 are used in (45).

Note that our collision triangle derivation automatically contains the gravity. That is, the desired flight path angle has been computed using a point mass model that already considers gravity and therefore we only need to use $\dot{\gamma} = a_M/V_M$ in guidance law design.

B. Optimal Guidance Law Design

In order to drive the interceptor onto the desired collision triangle, our objective here is to design an optimal guidance law that can force the instantaneous ZEM to converge to zero in finite time. To realize this, we formulate the following finite-time optimal regulation problem

$$\min_{a_M} \; J = \frac{1}{2}\int_t^{t_f} R(\tau)\, a_M^2(\tau)\, d\tau \tag{46}$$

subject to

$$\begin{aligned} \dot{z} &= -a_M\left(t_{go} + \tfrac{a_x}{2V_M} t_{go}^2\right) \\ z(t_f) &= 0 \end{aligned} \tag{47}$$

where $R(t) > 0$ is an arbitrary weighting function.

Due to the nonlinearity of the ZEM dynamics, it is difficult to apply the standard optimal control theory to find the analytical guidance command. We thereby seek to solve the above optimal control problem through Schwarz's inequality approach [5]. Imposing the integration from t to t_f on both sides of (45) gives

$$z(t_f) - z(t) = \int_t^{t_f} a_M(\tau)\, b(\tau)\, d\tau \tag{48}$$

where $b(t) = -\left(t_{go} + \frac{a_x}{2V_M(t)} t_{go}^2\right)$.

Since $z(t_f) = 0$, introducing a slack variable $R(t)$ renders (48) to

$$-z(t) = \int_t^{t_f} b(\tau)\, R^{-1/2}(\tau)\, R^{1/2}(\tau)\, a_M(\tau)\, d\tau \tag{49}$$

Applying Schwarz's inequality to the preceding equation yields

$$[-z(t)]^2 \le \left[\int_t^{t_f} R^{-1}(\tau)\, b^2(\tau)\, d\tau\right]\left[\int_t^{t_f} R(\tau)\, a_M^2(\tau)\, d\tau\right] \tag{50}$$

Rewriting inequality (50) as

$$\frac{1}{2}\int_t^{t_f} R(\tau)\, a_M^2(\tau)\, d\tau \ge \frac{z^2(t)}{2\left[\int_t^{t_f} R^{-1}(\tau)\, b^2(\tau)\, d\tau\right]} \tag{51}$$

which gives a lower bound of the performance index. According to Schwarz's inequality, the equality of (51) holds if and only if there exists a constant k such that

$$a_M(t) = kR^{-1}(t)\,b(t) \tag{52}$$

Substitution of (52) into (49) results in

$$-z(t) = k\int_t^{t_f} R^{-1}(\tau)\,b^2(\tau)\,d\tau \tag{53}$$

Solving (53) for k gives

$$k = \frac{-z(t)}{\int_t^{t_f} R^{-1}(\tau)\,b^2(\tau)\,d\tau} \tag{54}$$

Substituting (54) into (52) gives the optimal command as

$$a_M(t) = -z(t)\left[\frac{R^{-1}(t)\,b(t)}{\int_t^{t_f} R^{-1}(\tau)\,b^2(\tau)\,d\tau}\right] \tag{55}$$

which gives a general gravity-assited optimal guidance command with an arbitrary weighting function.

In order to shape the guidance command, consider a time-to-go weighted weighting function $R(t) = 1/t_{go}^{\alpha}$ with $\alpha \geq 0$ [6]. Since the interceptor's velocity is time-varying, it is difficult to obtain the analytical solution of the guidance command. To address this problem, we will assume a constant-speed vehicle and update the velocity at every time instant when implementing the guidance law. Under this assumption, the final guidance command is given by

$$a_M(t) = \frac{N(t)\,z(t)}{t_{go}^2} \tag{56}$$

where

$$N(t) = (\alpha+3)\left(\frac{1+\frac{a_x}{2V_M}t_{go}}{1+\frac{\alpha+3}{\alpha+4}\frac{a_x}{V_M}t_{go}+\frac{\alpha+3}{\alpha+5}\left(\frac{a_x}{2V_M}t_{go}\right)^2}\right) \tag{57}$$

which reveals that the proposed guidance law can be viewed as a PNG-type with a time-varying navigation ratio. This fact implies the proposed guidance law holds similar characteristics as standard PNG.

The initial and final value of the navigation ratios are given by

$$N_0 = (\alpha+3)\left(\frac{1+\frac{a_x}{2V_M}t_f}{1+\frac{\alpha+3}{\alpha+4}\frac{a_x}{V_{M0}}t_f+\frac{\alpha+3}{\alpha+5}\left(\frac{a_x}{2V_{M0}}t_f\right)^2}\right), \quad N_f = \lim_{t\to t_f} N(t) = \alpha+3 \tag{58}$$

where V_{M0} denotes the initial vehicle speed.

For endo-atmospheric interception, the guidance command is directly given by (56). In the case of exo-atmospheric interception, the shear angle command is obtained from $\sin\alpha_M = a_M/a_x$.

Remark 3. Although the formulation of the proposed guidance law is entirely based on the 2-D engagement, the proposed approach can be easily extended to a 3-D scenario by using the well-known separation concept. In the realistic 3-D scenario, one can first decouple the homing kinematics into the horizontal one and the vertical one. The classical guidance law, i.e. PNG and G2C, can be utilized for the horizontal homing engagement and the proposed gravity-assisted guidance law is suitable for the vertical plane.

Remark 4. Since a numerical approach is leveraged to calculate the desired flight path angle at every instant of time, the time of computation of the proposed guidance command for online implementation is slightly larger than that of PNG and G2C. However, there are some additional ways that we can utilize to reduce the computational power. For example, when we compute the desired flight path angle, we can choose initial guess of flight path angle as previous value.

C. Relationships with Previous Guidance Laws

This subsection discusses the relationships between the proposed guidance law (56) and some previous guidance laws derived using ZEM concept. Fig. 3 presents different kinds of ZEMs that are used in PNG, G2C and the proposed guidance law design. The length of the green straight line $A-D$ is the ZEM for PNG, the length of the blue straight line $A-C$ the ZEM for G2C, and the length of the purple straight line $A-B$ the proposed instantaneous ZEM. One can clearly observe from Fig. 3 that the desired paths for both PNG and G2C are straight lines from the current point to the their corresponding PIP points while the desired trajectory of the proposed guidance law is a curved line.

(1) Relationships with PNG [1].

The behind idea of PNG is to generate a lateral acceleration to nullify the ZEM so as to follow a straight line interception course. To maintain the collision triangle, it is necessary to equalize between the distances travelled by the interceptor and the target perpendicular to the LOS. In PNG formulation, the assumptions regarding no axial acceleration and gravity are required. Under

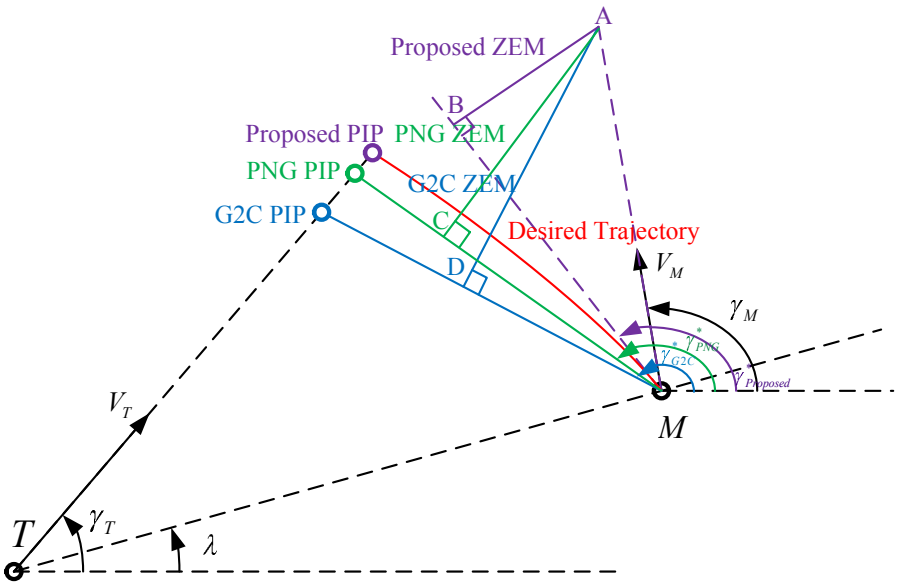

Fig. 3 Comparisons of different ZEMs in guidance law design.

these two assumptions, one can imply that

$$L_M \sin\left(\gamma_{PNG}^* - \lambda\right) - L_T \sin\left(\gamma_T - \lambda\right) = 0 \tag{59}$$

where γ_{PNG}^* denotes the desired current flight path angle of PNG. L_M and L_T are the vehicles' travelled distances from the current point to the PIP point.

Solving γ_{PNG}^* using (59) for the engagement case shown in Fig. 3 gives

$$\begin{aligned} \gamma_{PNG}^* &= \pi - \arcsin\left(\frac{L_T \sin(\gamma_T - \lambda)}{L_M}\right) + \lambda \\ &= \pi - \arcsin\left(\frac{V_T \sin(\gamma_T - \lambda)}{V_M}\right) + \lambda \end{aligned} \tag{60}$$

Then, the ZEM dynamics of PNG can be obtained as

$$z_{PNG} = -\sin\left(e_{\gamma,PNG}\right) V_M t_{go} \tag{61}$$

$$\dot{z}_{PNG} = -\dot{e}_{\gamma,PNG} V_M t_{go} = -a_M t_{go} \tag{62}$$

where $e_{\gamma,PNG} = \gamma_M - \gamma_{PNG}^*$ denotes the flight path angle tracking error.

Note that the difference between the PNG ZEM and the proposed ZEM is that the desired flight path angle for the former one is derived based on the assumption of constant flight velocity under the gravity-free condition, whereas the latter one computes it under the influence of gravity

for varying-speed missiles. The preceding PNG ZEM dynamics also reveals that if we remove the gravity and axial acceleration, the proposed instantaneous ZEM reduces to the PNG ZEM.

Following the optimal solutions shown in the previous subsection, one can easily derive the optimal part of PNG guidance command as

$$a_M^{op}(t) = \frac{(\alpha+3)\, z_{PNG}}{t_{go}^2} \tag{63}$$

Note that the optimal part of PNG has an equivalent form as $a_M^{op}(t) = (\alpha+3)\, V_c \dot{\lambda}$ with V_c being the closing velocity and hence the implementation of PNG requires no information on the time-to-go. Since classical PNG leverages the ZEM that is derived based on $g = 0$, it requires extra term $g\cos\gamma_M$ to compensate the gravity in implementation as

$$a_M(t) = a_M^{op}(t) + g\cos\gamma_M = \frac{(\alpha+3)\, z_{PNG}}{t_{go}^2} + g\cos\gamma_M \tag{64}$$

As a comparison, our ZEM derivation automatically considers the gravitational effect, and thereby the guidance command converges to zero once the interceptor is maintained on the collision triangle. In other words, our objective is to use, instead of reject, the gravity in terminal guidance.

(2) Relationships with G2C law [7–10].

Similar to PNG, the guidance goal of G2C is to maintain a straight line interception for intercepting targets. At any time instant during the interception, equalizing between the distances traveled by the interceptor and the target perpendicular to the LOS gives

$$L_M \sin(\gamma_{G2C}^* - \lambda) - L_T \sin(\gamma_T - \lambda) = 0 \tag{65}$$

where γ_{G2C}^* denotes the desired current flight path angle of G2C.

For constant accelerating missile and $g = 0$, (65) can be re-formulated as

$$\left(V_M + \frac{1}{2} a_M t_{go}\right) \sin(\gamma_{G2C}^* - \lambda) - V_T \sin(\gamma_T - \lambda) = 0 \tag{66}$$

Once a straight line collision course is reached and maintained after the heading error has been nulled, the time-to-go for G2C law can then be computed by [11]

$$r = V_T t_{go} \cos(\gamma_T - \lambda) + V_M t_{go} \cos[\pi - (\gamma_{G2C}^* - \lambda)] + \frac{1}{2} a_M t_{go}^2 \cos[\pi - (\gamma_{G2C}^* - \lambda)] \tag{67}$$

Solving γ^*_{G2C} using (66) for the engagement case shown in Fig. 3 gives

$$\gamma^*_{G2C} = \pi - \arcsin\left(\frac{V_T \sin(\gamma_T - \lambda)}{V_M + 0.5 a_M t_{go}}\right) + \lambda \tag{68}$$

Then, one can derive the G2C ZEM dynamics as

$$z_{G2C} = -\sin(e_{\gamma,G2C})\left(V_M t_{go} + \frac{1}{2} a_x t_{go}^2\right) \tag{69}$$

$$\dot{z}_{G2C} = -\dot{e}_{\gamma,G2C}\left(V_M t_{go} + \frac{1}{2} a_x t_{go}^2\right) = -a_M\left(t_{go} + \frac{a_x}{2V_M} t_{go}^2\right) \tag{70}$$

where $e_{\gamma,G2C} = \gamma_M - \gamma^*_{G2C}$ denotes the flight path angle tracking error.

The preceding two equations reveal that if we remove the gravity, the proposed instantaneous ZEM reduces to the G2C ZEM. Therefore, by replacing γ^* with γ^*_{G2C} in (44), our approach directly transforms to optimal G2C law without consideration of gravity. Following the same line shown in the previous subsection, one can easily verify that the optimal part of G2C is given by

$$a_M^{op}(t) = \frac{N(t)\, z_{G2C}}{t_{go}^2} \tag{71}$$

Similarly, as the ZEM of G2C is valid only for gravity-free case, one requires an additional gravity compensation term in the implementation of G2C as

$$a_M(t) = a_M^{op}(t) + g\cos\gamma_M = \frac{N(t)\, z_{G2C}}{t_{go}^2} + g\cos\gamma_M \tag{72}$$

Since the proposed guidance law utilizes gravity instead of compensating it, one can safely predict that our approach can save energy in the case of instantaneous ZEM$\leq$G2C ZEM. Furthermore, if we set $\alpha = 0$ and $g = 0$, then, (56) becomes

$$a_M(t) = \frac{3z(t)}{t_{go}^2}\left(\frac{4V_M + 2a_x t_{go}}{4V_M + 3a_x t_{go} + \frac{12}{5} V_M \left(\frac{a_x}{2V_M} t_{go}\right)^2}\right) \tag{73}$$

We further assume that a_x/V_M is a small variable. Under this condition, guidance command (73) can then be approximated as

$$a_M(t) = \frac{3z(t)}{t_{go}^2}\left(\frac{4V_M + 2a_x t_{go}}{4V_M + 3a_x t_{go}}\right) \tag{74}$$

which coincides with the energy optimal G2C law for endo-atmospheric interception [8] in ZEM format.

Table 1 Relationships between the proposed formulation and previous guidance laws.

Guidance Law	Guidance Command	Terminal Guidance Command	Consideration
PNG	$a_M(t) = \frac{(\alpha+3)z_{PNG}}{t_{go}^2} + g\cos\gamma_M$	Bounded	None
G2C	$a_M(t) = \frac{N(t)z_{G2C}}{t_{go}^2} + g\cos\gamma_M$	Bounded	Speed variation
Proposed	$a_M(t) = \frac{N(t)z_{Proposed}}{t_{go}^2}$	Zero	Speed variation and gravity

Table 1 summarizes the aforementioned relationships between the proposed guidance law and PNG as well as G2C. In conclusion, our approach is a more generalized guidance law derived from the collision triangle and the gravity effect is automatically considered in the instantaneous ZEM. As we stated earlier, the advantages of using gravity turn in guidance law design are that the guidance command can converge to zero at the time of impact and no extra energy for gravity compensation is required. This strategy can provide some additional margins to cope with the undesired disturbances.

D. Extensions to Intercept Angle Control

Although the proposed approach is considered only for homing case in the previous sections, this subsection shows that the proposed guidance law can be easily extended to intercept angle control. Constraining the intercept angle is often desirable in terms of increasing the warhead effectiveness as well as the kill probability for tactical missiles since it enables the interceptor to attack a vulnerable spot on a target [15–21]. In this paper, we denote the intercept angle as the missile's flight path angle at the time of impact. Generally, intercept angle control is an under actuation control problem, in which two constraints (zero ZEM and zero intercept angle error) are required to be satisfied with only one control input a_M. To address this problem, a guidance law providing zero ZEM in conjunction with an additional command term nullifying the intercept angle error is considered here. The proposed guidance law for intercept angle control is given by

$$a_M = a_{M0} + a_{bias} \tag{75}$$

where a_{M0} denotes the original guidance law (56) for nullifying the instantaneous ZEM and a_{bias} is a biased term to control the intercept angle.

The key problem of intercept angle control is to find the relationship between γ_{Mf} and a_M. This can be achieved by substituting (56) and (75) into (8) or (10). However, due to the complicated form of the time-varying navigation gain, it is intractable to find the analytical solution of the predicted final flight path angle due to biased guidance law (75). To this end, we will seek to find an approximated solution in this subsection.

As the original guidance law a_{M0} forces the missile to converge to the collision triangle defined by (34)-(40), a_{M0} never affect the intercept angle dynamics when the missile is maintained onto the desired collision triangle, i.e. the change rate of γ_{Mf} resulted from a_{M0} can be approximated as zero. Moreover, as the original guidance law a_{M0} is a PNG-like law with a time-varying navigation ratio, guidance law (75) can be viewed as a generalized biased PNG with a time-varying navigation gain. In [22], the authors revealed that the dynamics of γ_{Mf} caused by the biased term a_{bias} for fixed-gain PNG has the form

$$\dot{\gamma}_{Mf} = -\frac{a_{bias}}{(N-1)\,V_M} \tag{76}$$

Motivated by (76), one can then find an approximated relationship between γ_{Mf} and a_{bias} in our case as

$$\dot{\gamma}_{Mf} \approx -\frac{a_{bias}}{(N(t)-1)\,V_M(t)} \tag{77}$$

Let γ_f be the desired final flight path angle of the missile and denote the final flight path angle error as $\varepsilon_\gamma = \gamma_f - \gamma_{M_f}$. Then, one can imply that

$$\dot{\varepsilon}_\gamma \approx \frac{a_{bias}}{[N(t)-1]\,V_M(t)} \tag{78}$$

In order to find the analytical solution of the guidance command, we assume both the speed of the vehicle and the navigation gain are instantaneous constant at each time instant. We update these two variables at every time instant when implementing the guidance law. Considering a time-to-go weighted weighting function $R(t) = 1/t_{go}^{K-1}$ with $K \geq 1$ and following the same line as shown in (46)-(55), one can obtain the optimal biased term as

$$a_{bias} = -\frac{K\,[N(t)-1]\,V_M(t)}{t_{go}}\varepsilon_\gamma \tag{79}$$

Table 2 Initial conditions for homing engagement.

Parameters	Values
Missile-target initial relative range, $r(0)$	$50km$
Initial LOS angle, $\lambda(0)$	0°
Missile initial velocity, $V_M(0)$	$1500m/s$
Target velocity, V_T	$3000m/s$
Interceptor's axial acceleration, a_x	$20g$

Consequently, the intercept angle control guidance law for accelerating missiles in the presence of gravity is formulated as

$$a_M(t) = \frac{N(t)\, z(t)}{t_{go}^2} - \frac{K\left[N(t)-1\right] V_M(t)}{t_{go}} \varepsilon_\gamma \tag{80}$$

Note that although we leverage an approximated dynamics (77) for finding the analytical solution of the guidance command, we never use dynamics (77) in predicting the final flight path angle. Actually, the predicted final flight path angle γ_{M_f} is obtained by solving the coupled equations in (43). As the two equations in (43) are closed-form formulations without any assumptions, the predicted final flight path angle is accurate enough in terms of practical applications. Furthermore, the error feedback term in (80) can still further reduce the effect of the approximating error of (77).

V. Simulation Results

In this section, nonlinear simulations are performed to validate the proposed guidance law. We first apply our guidance law to exo-atmospheric interception under various conditions to analyze its characteristics and then compare our approach with other guidance laws. The required initial conditions for a typical exo-atmospheric engagement, taken from [8, 10], are summarized in Table 2.

A. Characteristics of the Proposed Guidance Law

This subsection investigates the characteristics of the proposed guidance law (56). We first analyze the effect of guidance gain α on the guidance performance. In the simulations, the initial conditions are chosen as: $\gamma_M(0) = 150^\circ$ and $\gamma_T(0) = 20^\circ$. The simulation results, including

interception trajectory, shear angle command, flight path angle error, control effort, time-to-go estimation and missile velocity, with various guidance gains $\alpha = 4, 6, 8, 10, 12$ are presented in Fig. 4, where the control effort is defined as $\int_0^t a_M^2(\tau)\, d\tau$. The results in this figure clearly reveal that guidance law (56) with larger guidance gain α results in faster convergence speed of the flight path angle error. Large guidance gain, in turn, also requires higher shear angle command during the initial flight period, thereby generating more control effort. When the flight path angle tracking error is close to zero, the control effort almost remains the same and the shear angle commands are also close to zero for all guidance gain cases, meaning that the interceptor is maintained on the collision triangle. Since we directly adopt the gravity in collision triangle derivation, the guidance command converges to zero at the time of impact with the increasing of the guidance gain. This characteristic is totally different from previous guidance laws that used an additional term $g\cos\gamma_M$ to compensate the gravity. The results in Figs. 4 (e) our closed-form solution gives accurate estimation of the time-to-go and the estimation error converges to zero once the interceptor is maintained on the desired trajectory. From the zoomed-in subfigure in Fig. 4 (f), one can observe that the missile velocity with smaller guidance gain α increases slightly faster than that with larger guidance gain α during the initial flight phase. The reason of this phenomenon is that larger guidance gain requires more control effort, i.e. larger magnitude of the shear angle. Since the shear angle remains very small during most of the flight period, the missile velocity in the considered scenario increases almost linearly, as shown in Fig. 4 (f).

Next, we perform simulations to investigate the guidance performance under different interceptor's initial flight path angles. The same scenario is simulated with four different values of $\gamma_M(0) = 90^\circ, 120^\circ, 150^\circ, 180^\circ$ and $\gamma_T(0) = 20^\circ$. The simulation results with guidance gain $\alpha = 6$ are depicted in Fig. 5. Obviously, the missile successfully intercept the target following the desired collision triangle in all cases. The more the interceptor deviates from the desired path, the more curved trajectory the missile generates during the initial flight period. For this reason, the duration of initial acceleration saturation of $\gamma_M(0) = 180^\circ$ is longer than that of other cases. As the proposed time-to-go is calculated from the desired collision triangle, it gives an underestimation when flight path angle error exists. However, the estimation accuracy is still acceptable in most cases. From

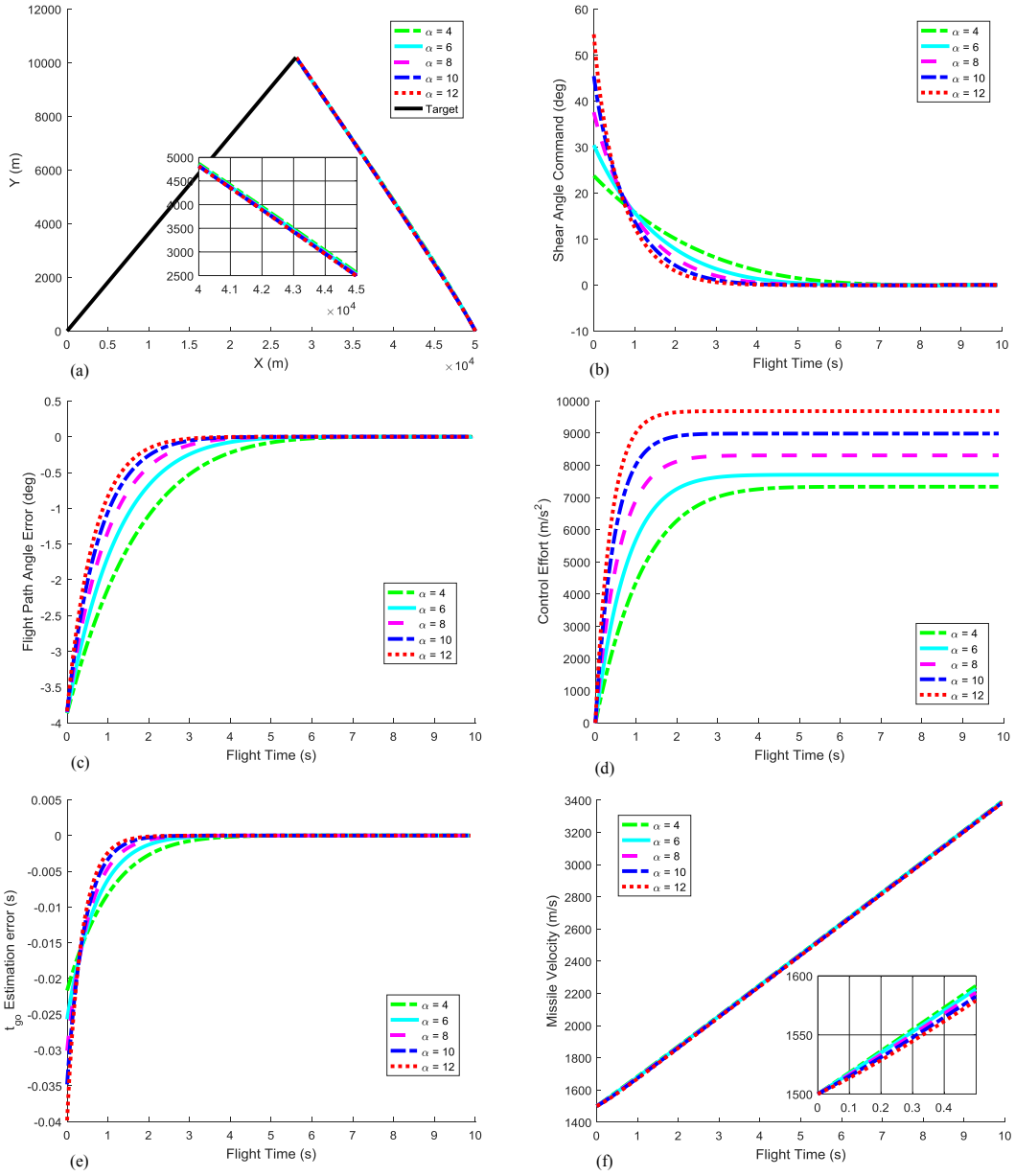

Fig. 4 Simulation results of the proposed guidance law (56) with different guidance gains: (a) interception trajectory; (b) shear angle command; (c) flight path angle error; (d) control effort; (e) time-to-go estimation; and (f) missile velocity.

Fig. 5 (f), it can be noted that the missile velocity deceases slightly due to the gravitational effect when the guidance command is saturated and all control effort is used to nullify the instantaneous ZEM.

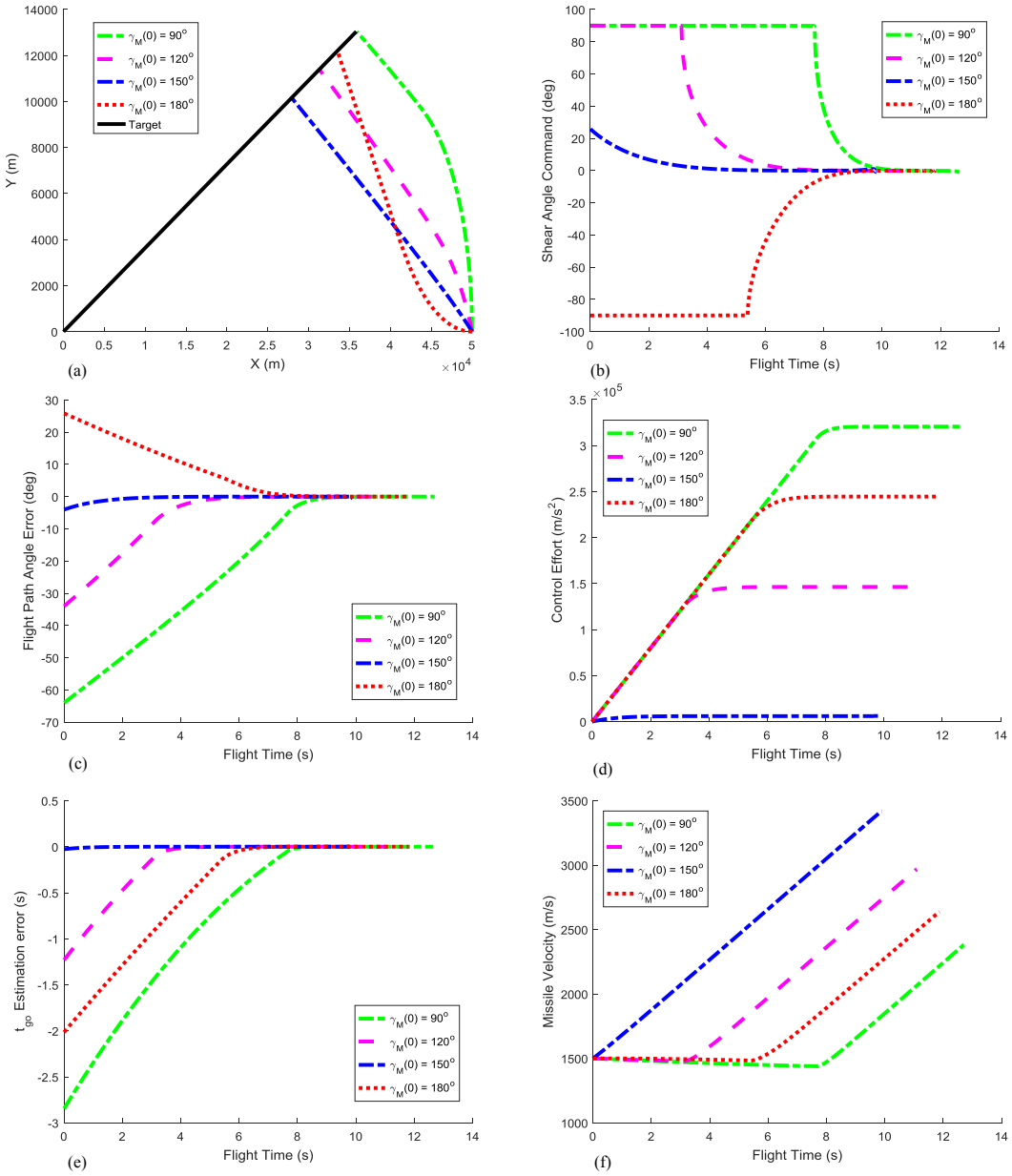

Fig. 5 Simulation results of the proposed guidance law (56) with different initial flight path angles: (a) interception trajectory; (b) shear angle command; (c) flight path angle error; (d) control effort; (e) time-to-go estimation; and (f) missile velocity.

B. Comparison with Other Guidance Laws

To further demonstrate the superiority of the proposed approach, the performance of our new guidance law is compared to that of classical PNG and G2C in this subsection. In the simulations, we use the well-known approach by adding an additional term $g\cos\gamma_M$ in both PNG and G2C to compensate the gravity. In order to make fair comparisons, the guidance gain for all guidance

Table 3 Mean miss distances of three different guidance laws.

	PNG	G2C with gravity compensation	G2C using gravity
Mean miss distance	$0.32m$	$0.18m$	$0.18m$

laws is set as $\alpha = 6$. For the purpose of comparison, we call previous G2C as G2C with gravity compensation and our guidance law as G2C using gravity. In this subsection, the initial conditions are chosen as: $\gamma_M(0) = 150^\circ$ and $\gamma_T(0) = 20^\circ$.

Fig. 6 compares the performance of these three guidance laws for intercepting a non-maneuvering target. From this figure, it can be noted that the axial acceleration of PNG does not align with the velocity vector, thereby forcing the missile to fly along a curved path to intercept the target. Unlike PNG, G2C with gravity compensation hits the target following a straight line after the initial heading error is nullified. As a comparison, our G2C using gravity follows a slightly curved trajectory as we intend to exploit the gravity-turn. It is evident from Fig. 5 (b) that the time evolutions of shear angle of all guidance laws remain bounded and the proposed law guarantees zero guidance command at the time of impact. Therefore, the proposed guidance law holds additional trajectory shaping ability to provide more operational margins than previous G2C law when the missile approaches the target. Since the proposed guidance law requires no extra term to counteract the gravity, one can clearly observe from Fig. 6 (b) that our approach saves the energy consumption during the terminal guidance phase. The ZEM profiles, shown in Fig. 6 (c), reveal that all three guidance laws can regulate their corresponding ZEM to zero to guarantee the interception. Since the magnitude of the instantaneous ZEM is less than that of the ZEM under G2C with gravity compensation, the proposed gravity turn-assisted optimal guidance law requires less control effort than classical G2C law and thus can save energy consumption. From Fig. 6 (d), one can observe that both the proposed guidance law and previous G2C law have larger terminal velocity, thereby enabling higher kill probability than PNG law. Table 3 summarizes the mean miss distances of these three different guidance laws in 100 Monte-Carlo simulations. It is clear that both G2C laws exhibit better homing performance than the classical PNG law.

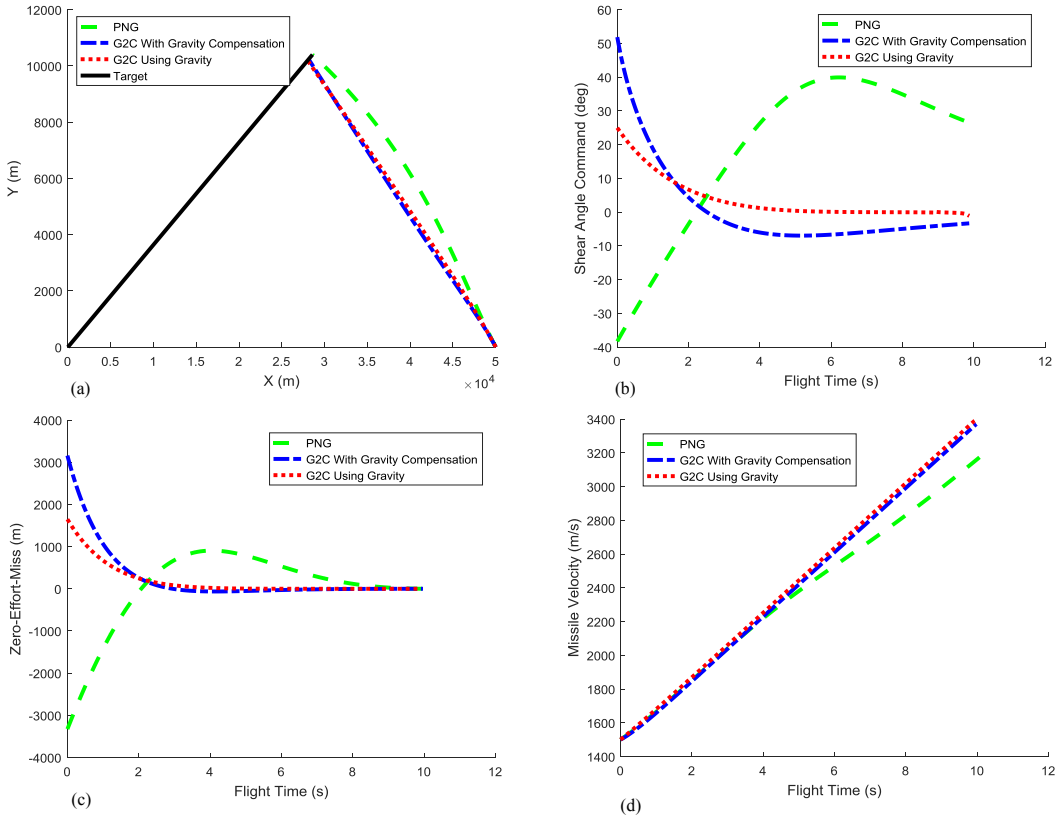

Fig. 6 Comparison results of exo-atmospheric interception with a non-maneuvering target: (a) interception trajectory; (b) shear angle command; (c) zero-effort-miss; and (d) missile velocity.

C. Performance of the Proposed Intercept Angle Guidance Law

This subsection verifies the proposed intercept angle guidance law (80) in the same exo-atmospheric interception scenario against a constant moving target. The desired final flight path angle is set as $\gamma_f = 160^\circ$ and the guidance gain to regulate the flight path angle error is selected as $K = 6$. Fig. 7 (a) presents the interception trajectories for different initial flight path angles, demonstrating that the proposed guidance law successfully captures the target in all cases. The shear angle guidance command is shown in Fig. 7 (b), which clearly reveals that the guidance command converges to zero at the time of impact. Since the missile with $\gamma_M(0) = 90^\circ$ is highly deviated from the desired collision triangle, more control effort is required to correct the flight trajectory. Fig. 7 (c) compares the time evolution of the flight path angle of all conditions. One can obviously note from this figure that the flight path angle gradually converges to the desired

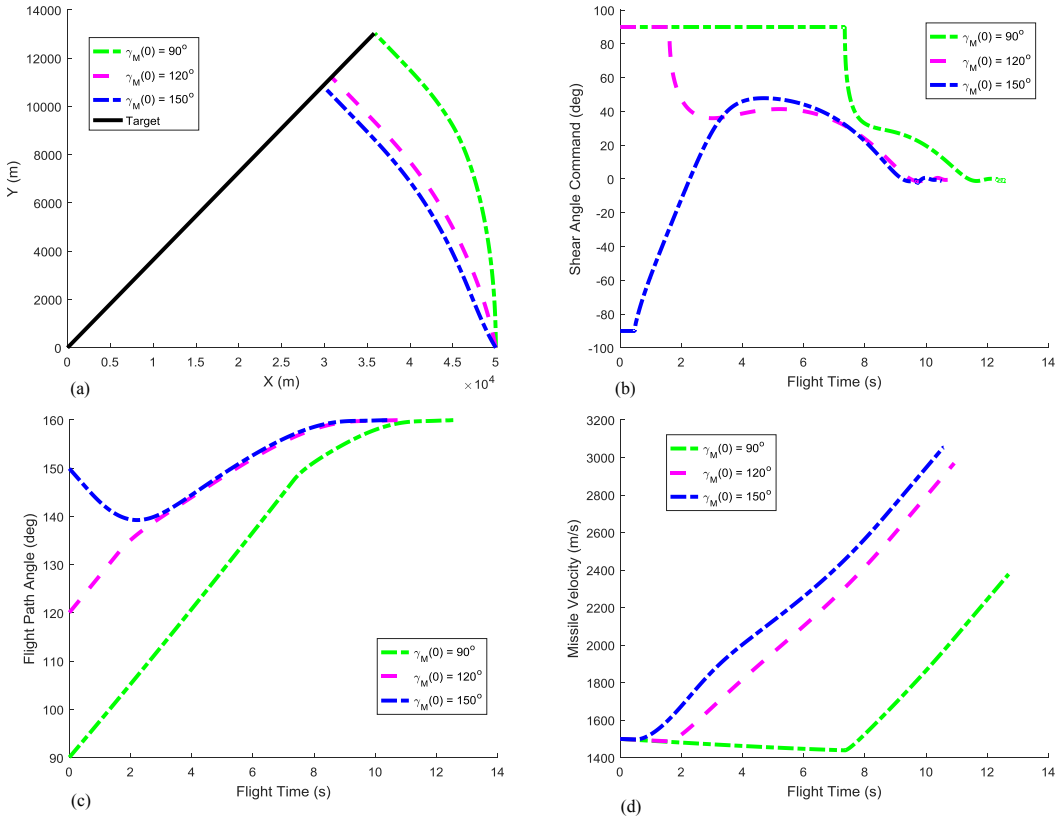

Fig. 7 Simulation results of the proposed guidance law (80) with initial flight path angles: (a) interception trajectory; (b) shear angle command; (c) flight path angle; and (d) missile velocity.

value when the interceptor approaches the target. Fig. 7 (d) depicts the missile velocity profile for various initial flight path angles. This figure reveals that, once the interceptor is forced onto the desired collision course, the vehicle flying velocity increases linearly as time goes.

VI. Conclusion

The problem of optimal guidance law design for accelerating missiles in the presence of gravity is investigated in this paper. The proposed guidance law is derived based on a new concept, called instantaneous ZEM, and Schwarz's inequality. The key feature of the proposed guidance law lies in that it automatically leverages the gravitational acceleration. The benefits of using gravity are clear: guaranteeing zero final guidance command and saving energy. We also show that the conventional PNG and G2C are special cases of the proposed guidance law.

The proposed results are believed to have an academic significance as well as a practical one

since it suggests a new way to utilize gravity in guidance law design. By using the proposed results, one can also exploit the advantages of gravity turn in midcourse guidance law design.

Appendix A. Closed-Form Solution of (24)-(26)

Noting from (24)-(26) that the solution requires the integration of $h(\gamma_M)(\sec\gamma_M+\tan\gamma_M)^n$, where $h(\gamma_M)$ is a function of secant and tangent functions. For an arbitrary function $\beta(\gamma_M)$, we have

$$\begin{aligned}&\tfrac{d}{d\gamma_M}\left[\beta(\gamma_M)(\sec\gamma_M+\tan\gamma_M)^n\right]\\&\quad=\tfrac{d\beta(\gamma_M)}{d\gamma_M}(\sec\gamma_M+\tan\gamma_M)^n+n\beta(\gamma_M)\left(\sec\gamma_M\tan\gamma_M+\sec^2\gamma_M\right)\\&\quad=\left(\tfrac{d\beta(\gamma_M)}{d\gamma_M}+n\beta(\gamma_M)\sec\gamma_M\right)(\sec\gamma_M+\tan\gamma_M)^n\end{aligned}\tag{81}$$

which reveals that the general solution of $\int h(\gamma_M)(\sec\gamma_M+\tan\gamma_M)^n d\gamma_M$ can be obtained by equalizing $h(\gamma_M)$ and $\frac{d\beta(\gamma_M)}{d\gamma_M}+n\beta(\gamma_M)\sec\gamma_M$.

On the basis of the properties of secant and tangent functions, the function $\beta(\gamma_M)$ for solving (24)-(26) has the form

$$\beta(\gamma_M)=a_1\sec\gamma_M+a_2\tan\gamma_M+a_3\sec^2\gamma_M+a_4\tan^2\gamma_M+a_5\sec\gamma_M\tan\gamma_M\tag{82}$$

where a_i, $i=1,2,3,4,5$ are constant coefficients to be determined.

Differentiating (82) with respect to γ_M gives

$$\begin{aligned}\tfrac{d\beta(\gamma_M)}{d\gamma_M}&=a_1\sec\gamma_M\tan\gamma_M+a_2\sec^2\gamma_M+2a_3\sec^2\gamma_M\tan\gamma_M\\&\quad+2a_4\sec^2\gamma_M\tan\gamma_M+a_5\left(\sec\gamma_M\tan^2\gamma_M+\sec^3\gamma_M\right)\end{aligned}\tag{83}$$

Substituting (82) and (83) into (81) yields

$$\begin{aligned}\tfrac{d}{d\gamma_M}\left[\beta(\gamma_M)(\sec\gamma_M+\tan\gamma_M)^n\right]&=(na_1+a_2)\sec^2\gamma_M+(na_2+a_1)\sec\gamma_M\tan\gamma_M\\&\quad+(na_3+a_5)\sec^3\gamma_M+(na_4+a_5)\sec\gamma_M\tan^2\gamma_M+(na_5+2a_3+2a_4)\sec^2\gamma_M\tan\gamma_M\end{aligned}\tag{84}$$

For (24), we have $h(\gamma_M)=\sec^2\gamma_M$, $n=\kappa$. Using the coefficient comparison approach, the

following coupled equations hold

$$\begin{cases} \kappa a_1 + a_2 = 1 \\ \kappa a_2 + a_1 = 0 \\ \kappa a_3 + a_5 = 0 \\ \kappa a_4 + a_5 = 0 \\ \kappa a_5 + 2a_3 + 2a_4 = 0 \end{cases} \tag{85}$$

Solving (85) gives

$$a_1 = \frac{\kappa}{\kappa^2 - 1}, a_2 = -\frac{1}{\kappa^2 - 1}, a_3 = a_4 = a_5 = 0 \tag{86}$$

Then, the closed-form solution of (24) is given by

$$t(\gamma_M) = t(\gamma_{M0}) - \frac{C}{g}\left[f_t(\gamma_M) - f_t(\gamma_{M0})\right] \tag{87}$$

For (25), we have $h(\gamma_M) = \sec^2 \gamma_M$, $n = 2\kappa$. Replacing κ with 2κ in (85) leads to the closed-form solution of (25) as

$$x_M(\gamma_M) = x_M(\gamma_{M0}) - \frac{C^2}{g}\left[f_x(\gamma_M) - f_x(\gamma_{M0})\right] \tag{88}$$

For (26), we have $h(\gamma_M) = \sec^2 \gamma_M \tan \gamma_M$, $n = 2\kappa$. Using the coefficient comparison approach, the following coupled equations hold

$$\begin{cases} \kappa a_1 + a_2 = 0 \\ \kappa a_2 + a_1 = 0 \\ \kappa a_3 + a_5 = 0 \\ \kappa a_4 + a_5 = 0 \\ \kappa a_5 + 2a_3 + 2a_4 = 1 \end{cases} \tag{89}$$

Solving (89) gives

$$a_1 = a_2 = 0, a_3 = -\frac{1}{\kappa^2 - 4}, a_4 = -\frac{1}{\kappa^2 - 4}, a_5 = \frac{\kappa}{\kappa^2 - 4} \tag{90}$$

which gives the closed-form solution of (26) as

$$y_M(\gamma_M) = y_M(\gamma_{M0}) - \frac{C^2}{g}\left[f_y(\gamma_M) - f_y(\gamma_{M0})\right] \tag{91}$$

References

[1] P. Zarchan, *Tactical and Strategic Missile Guidance*, fifth Edition, Washington, DC: AIAA, 2007.

[2] S. A. Murtaugh and H. E. Criel, "Fundamentals of proportional navigation," *IEEE Spectrum*, vol. 3, no. 12, pp. 75–85, 1966.

[3] N. F. Palumbo, R. A. Blauwkamp, and J. M. Lloyd, "Basic principles of homing guidance," *Johns Hopkins APL Technical Digest*, vol. 29, no. 1, pp. 25–41, 2010.

[4] I. S. Jeon and J. I. Lee, "Optimality of proportional navigation based on nonlinear formulation," *IEEE Transactions Aerospace and Electronic Systems*, vol. 46, no. 4, pp. 2051–2055, 2010.

[5] C. H. Lee, M. J. Tahk, and J. I. Lee, "Generalized formulation of weighted optimal guidance laws with impact angle constraint," *IEEE Transactions on Aerospace and Electronic Systems*, vol. 49, no. 2, pp. 1317-1-322, 2013.

[6] C. K. Ryoo, H. Cho, and M. J. Tahk, "Time-to-go Weighted Optimal Guidance with Impact Angle Constraints," *IEEE Transactions on Control System Technology*, vol. 14, no. 3, pp. 483–492, 2006.

[7] R. Gazit, "Guidance to Collision of a Variable-Speed Missile," *Proceedings of the 1st IEEE Regional Conference on Aerospace Control Systems*, pp. 734–737, 1993.

[8] R. Gazit and S. Gutman,, "Development of Guidance Laws for a Variable-Speed Missile," *Dynamics and Control*, vol. 1, no. 2, pp. 177–198, 1991.

[9] T. Shima and O. Golan, "Exo-Atmospheric Guidance of an Accelerating Interceptor Missile," *Journal of the Franklin Institute*, vol. 349, no. 2, pp. 622–637, 2012.

[10] T. Shima and J. Shinar, "Time-varying linear pursuit-evasion game models with bounded controls," *Journal of Guidance, Control, and Dynamics*, vol. 25, no. 3, pp. 425–432, 2002.

[11] D. Reisner and T. Shima, "Optimal Guidance-to-Collision Law for an Accelerating Exoatmospheric Interceptor Missile," *Journal of Guidance, Control, and Dynamics*, vol. 36, no. 6, pp. 1695–1708, 2013.

[12] R. Padhi, and M. Kothari, "Model predictive static programming: a computationally efficient technique for suboptimal control design," *International Journal of Innovative Computing, Information and Control*, vol. 5, no. 2, pp. 399–411, 2009.

[13] A. R. Conn, N. I. Gould, and P. L. Toint, *Trust region methods*, Philadelphia: Society for Industrial and Applied Mathematics, 2001.

[14] C. Kanzow, N. Yamashita, and M. Fukushima M, "LevenbergâĂŞMarquardt methods with strong local convergence properties for solving nonlinear equations with convex constraints," *Journal of Computational and Applied Mathematics*, vol. 172, no. 2, pp. 375–397, 2004.

[15] P. Lu, D. B. Doman, and J. D. Schierman, "Adaptive Terminal Guidance for Hypervelocity Impact in Specified Direction," *Journal of Guidance, Control, and Dynamics*, vol. 29, no. 2, pp. 269–278, 2006.

[16] A. Ratnoo and D. Ghose, "Impact Angle Constrained Interception of Stationary Targets," *Journal of Guidance, Control, and Dynamics*, vol. 31, no. 6, pp. 1816–1821, 2008.

[17] R. Tekin and K. S. Erer, "Switched-Gain Guidance for Impact Angle Control Under Physical Constraints," *Journal of Guidance, Control, and Dynamics*, vol. 38, no. 2, pp. 205–216, 2015.

[18] H. B. Oza and R. Padhi, "Impact-angle-constrained suboptimal model predictive static programming guidance of air-to-ground missiles," *Journal of Guidance, Control, and Dynamics*, vol. 35, no. 1, pp. 153–164, 2012.

[19] I. Rusnak, H. Weiss, R. Eliav, and T. Shima, "Missile guidance with constrained intercept body angle," *IEEE Transactions on Aerospace and Electronic Systems*, vol. 50, no. 2, pp. 1445–1453, 2014.

[20] V. Shaferman and T. Shima, "Linear Quadratic Guidance Laws for Imposing a Terminal Intercept Angle," *Journal of Guidance, Control, and Dynamics*, vol. 31, no. 5, pp. 1400–1412, 2008.

[21] S. R. Kumar, S. Rao, and D. Ghose, "Sliding-mode guidance and control for all-aspect interceptors with terminal angle constraints," *Journal of Guidance, Control, and Dynamics*, vol. 35, no. 4, pp. 1230–1246, 2012.

[22] C. H. Lee, T. H. Kim, and M. J. Tahk, "Interception Angle Control Guidance using Proportional Navigation with Error Feedback," *Journal of Guidance, Control, and Dynamics*, vol. 36, no. 5, pp. 1556–1561, 2013.

2017-07-31

Gravity-turn-assisted optimal guidance law

He, Shaoming

AIAA

Shaoming He and Chang-Hun Lee. Gravity-turn-assisted optimal guidance law. Journal of Guidance, Control, and Dynamics, Vol. 41, Issue 1, 2018, pp. 171-183
http://dx.doi.org/10.2514/1.G002949